



**On the Physical Basis for the Swelling Resistance
of Ferritic Steels**

J. Sniegowski and W.G. Wolfer

August 1983

UWFDM-535

Presented at the AIME Conference on Ferritic Alloys for Use in Nuclear Energy
Technologies, June 19-23, 1983, Snowbird, Utah.

FUSION TECHNOLOGY INSTITUTE

UNIVERSITY OF WISCONSIN

MADISON WISCONSIN

DISCLAIMER

This report was prepared as an account of work sponsored by an agency of the United States Government. Neither the United States Government, nor any agency thereof, nor any of their employees, makes any warranty, express or implied, or assumes any legal liability or responsibility for the accuracy, completeness, or usefulness of any information, apparatus, product, or process disclosed, or represents that its use would not infringe privately owned rights. Reference herein to any specific commercial product, process, or service by trade name, trademark, manufacturer, or otherwise, does not necessarily constitute or imply its endorsement, recommendation, or favoring by the United States Government or any agency thereof. The views and opinions of authors expressed herein do not necessarily state or reflect those of the United States Government or any agency thereof.

**On the Physical Basis for the Swelling
Resistance of Ferritic Steels**

J. Sniegowski and W.G. Wolfer

Fusion Technology Institute
University of Wisconsin
1500 Engineering Drive
Madison, WI 53706

<http://fti.neep.wisc.edu>

August 1983

UWFDM-535

Presented at the AIME Conference on Ferritic Alloys for Use in Nuclear Energy Technologies, June 19-23, 1983, Snowbird, Utah.

ON THE PHYSICAL BASIS FOR THE SWELLING RESISTANCE OF FERRITIC STEELS

J.J. Sniegowski and W.G. Wolfer

Fusion Engineering Program
Nuclear Engineering Department
University of Wisconsin-Madison
Madison, Wisconsin 53706

August 1983

UWFD-535

Presented at Ferritic Alloys for Use in Nuclear Energy Technologies Conf.,
Snowbird, Utah, June 19-23, 1983.

ON THE PHYSICAL BASIS FOR THE SWELLING RESISTANCE OF FERRITIC STEELS

J.J. Sniegowski and W.G. Wolfer

Fusion Engineering Program, Nuclear Engineering Department
University of Wisconsin, Madison, Wisconsin 53706, U.S.A.

The swelling behavior of austenitic and ferritic alloys is briefly reviewed and the hypothesis is advanced that a fundamental difference exists between these two alloy classes which originates from the difference in the net bias. Since the net bias depends most critically on the relaxation volumes of interstitials and vacancies, experimental and theoretical values are discussed and reviewed. It is shown that the interstitial relaxation volume for fcc metals is almost twice as large as its value for bcc metals, whereas the reverse is true for the vacancy relaxation volume.

In order to obtain the net bias, the bias factors of voids and dislocations for both interstitial and vacancy capture are required. Equations are given for these bias factors and the net bias is computed. Due to the difference in the relaxation volumes in the austenitic and the ferritic structure, the net bias is large in austenitic alloys and significantly less in ferritic alloys. Using an upper bound for the void swelling rate, it is shown that austenitic alloys may exhibit a maximum swelling rate of about 1.4%/dpa,

whereas ferritic alloys are estimated to possess a maximum swelling rate of about 0.2%/dpa.

1. Introduction

The experimental evidence on swelling in ferritic and austenitic alloys as shown in Fig. 1 suggests that there is a fundamental difference between the two classes of alloys with regard to their propensity for void formation under irradiation. Whereas the latter class exhibits, after an incubation period of low swelling, a steady state swelling rate on the order of 1%/dpa, the former class has either a much longer incubation period, a much lower rate for steady-state swelling, or both. Unfortunately, the experimental data accumulated so far for ferritic alloys allow only one unambiguous conclusion to be drawn: namely that the incubation period is long in comparison to most austenitic alloys. Although there still exists the possibility that ferritic alloys may eventually swell at a significant rate we like to present theoretical arguments which indicate that the basic driving force for both void nucleation and growth is substantially

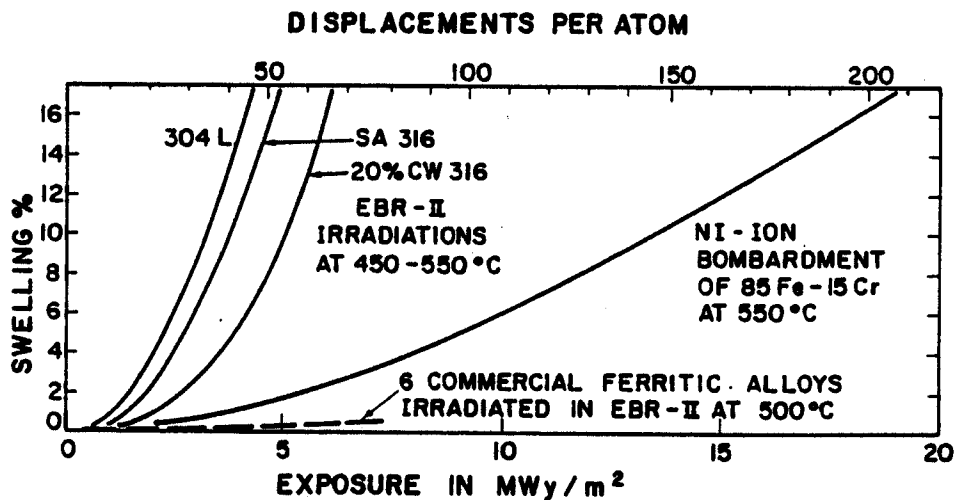


Fig. 1. Comparison of swelling for austenitic and ferritic alloys based on the following sources: 304 L -- swelling in annealed fuel capsules, Garner & Porter [1]; SA 316 and 20% CW 316 -- D0-heat irradiated in EBR-II and HFIR, Maziasz & Grossbeck [2], Brager & Garner [3]; 85 Fe-15 Cr -- Johnston, Lauritzen, Rosolowski & Turkalo [4]; ferritic alloys -- Powell, Peterson, Zimmerschied & Bates [5].

different in the two alloy classes. The difference originates at a fundamental level in connection with the relaxation volumes of self-interstitials and vacancies. Whereas in face-centered cubic metals the relaxation volume of an interstitial is large and that of a vacancy small, the body-centered cubic metals have smaller interstitial relaxation volumes but larger vacancy relaxation volumes. This results in a large net bias for the fcc metals but a small one for bcc metals. Accordingly, we suggest that this is one of the fundamental causes for the greater swelling resistance of bcc metals and alloys in general, and of ferritic alloys in particular.

We realize of course that there are other fundamental differences between the two crystal structures and their associated microstructures, and that these differences can further accentuate the dissimilarity in the swelling behavior. For example, martensitic and heat-treated steels contain very high densities of dislocations and boundaries in comparison to austenitic steels. As a result, point defect losses to these sinks are high in martensitic and many ferritic alloys. Furthermore, the friction stress for dislocation glide is also higher in bcc metals as compared to fcc metals, and this may result in a denser dislocation network produced during irradiation.

Other causes for the dissimilarity in swelling may arise from the precipitate structure. Due to the much lower solubility for interstitial elements in the ferrite phase and as a result of tempering and heat treatment, a high density of finely dispersed precipitate particles is often present in ferritic and tempered martensitic alloys. These precipitates may provide a high density of recombination sites. With all these factors compounded, the substantial difference in the swelling behavior of austenitic and ferritic alloys observed to date is not unexpected.

However, in view of the ultimate target exposure of about 400 to 600 dpa for first wall materials in fusion reactors, it is essential to find the causes of the swelling resistance of alloys and whether they are of an intrinsic and permanent nature or of a metallurgically-controlled and transitory kind.

Many of the microstructural differences mentioned above may not be stable under irradiation at elevated temperatures. For example, the high dislocation density in martensitic steels may eventually recover. The small carbide precipitates may be dissolved by high-energy collision cascades, and a coarser precipitate structure may form after prolonged irradiation. At temperatures around 400°C and higher, tempering of martensite eventually results in the formation of equi-axed ferrite grains. Therefore, at these elevated temperatures, the high sink density provided by the initial martensite boundaries may eventually be lost.

Therefore, the ultimate swelling resistance of all ferritic and martensitic alloys may in the final analysis depend only on the net bias. We consider this intrinsic property of the utmost importance.

For its evaluation in the following sections, the relaxation volumes of the self-interstitial and the vacancy are required. The experimental and theoretical results obtained for these volumes are reviewed in Section 2. Since the net bias depends on differences in bias factors for dislocations and voids, these factors and their determination will be reviewed in Section 3. Finally, numerical results for the net

bias are presented in Section 4 as a function of the point defect relaxation volumes.

2. Relaxation Volumes of Point Defects

The formation of point defects is accompanied by volume changes of the crystal lattice. These volume changes determine, at least to first order, the strength of the interaction with stress fields. By way of introducing the following notation, the definitions for different volumes associated with point defects are recapitulated.

A vacancy can be thought of as having been created by removing an atom from a regular lattice site and by depositing it on an external surface, a grain boundary, or into the core of an edge dislocation. The volume change connected with this process is referred to as the vacancy formation volume

$$\Delta V_V^f = v_V^f + \Omega, \quad (1)$$

where Ω is the atomic volume and v_V^f is the relaxation volume of the vacancy in its stable configuration. When the vacancy diffuses, the lowest possible activation energy for migration is realized in the saddle-point configuration for which the volume change is denoted by

$$\Delta V_V^S = v_V^S + \Omega = \Delta V_V^f + \Delta V_V^m \quad (2)$$

where ΔV_V^m is the activation volume for vacancy migration and ΔV_V^S is also referred to as the activation volume for self-diffusion. The latter can be determined experimentally by measuring the pressure dependence of the self-diffusion coefficient.

Formation and relaxation volumes for the self-interstitial are defined in an analogous manner. However, there occurs a change in sign when removing an atom from an external surface, a grain boundary, or from an edge dislocation core and inserting it interstitially into the lattice. Accordingly,

$$\Delta V_I^f = v_I^f - \Omega \quad (3)$$

and
$$\Delta V_I^S = v_I^S - \Omega = \Delta V_I^f + \Delta V_I^m. \quad (4)$$

The first-order interaction energy of a point defect with the hydrostatic stress field $\sigma_H(\vec{r})$ produced by a remote source is now given by $(-\sigma_H v)$ at all points in a solid except at locations which represent sinks or sources for point defects. At these points, the first-order interaction energy may be given by $(-\sigma_H \Delta V^f)$, depending on the sink type, its orientation with the applied stress, etc. For evaluating the equilibrium concentration of point defects and its dependence on stress, the interaction energy $(-\sigma_H \Delta V^f)$ is in general the relevant quantity. For bias calculations, however, the interaction energy $(-\sigma_H v^S)$ and the relaxation volume v^S in the saddle-point are the appropriate quantities.

Relaxation Volumes for Self-Interstitials

Relaxation volumes for self-interstitials in their stable configuration, i.e. v_I^f , can be determined from diffuse x-ray scattering and lattice parameter measurements on single crystals irradiated at liquid helium temperatures. A recent review of the results obtained by these techniques is given by Ehrhart [6], and his results are listed in Tables I and II.

It is generally believed that the relaxation volume of the self-interstitial in the saddle-point is very close to its value in the stable configuration. Experimental support for this conclusion is provided by the field-ion microscopy work of Seidman et al. [7]. According to these results, $\Delta V_I^m/\Omega < 0.03$ for Pt and $\Delta V_I^m/\Omega < 0.02$ for W.

The large values for the relaxation volume, v_I^f , in cubic metals can be rationalized in terms of the most efficient hard-sphere packing of the atoms which comprise the dumbbell interstitial and its next nearest neighbors. Based on this idea and Zener's approach to compute volume changes due to internal stresses, Wolfer [8] has developed a model for the relaxation volume of self-interstitials in cubic metals. Results of this model together with the experimentally obtained values are listed in Tables I and II for fcc and bcc metals, respectively.

It is seen from Table I that the theoretical results are in good agreement with the experimentally measured values in the case of fcc metals, and that the interstitial relaxation volume is around 1.8Ω .

For bcc metals, the results in Table II show that the relaxation volume is smaller by almost a factor of two. The theoretical values are close to the lower bound of the experimental range for the two metals where a comparison can be made, namely α -Fe and Mo.

Table I. Relaxation Volumes for Self-Interstitials in FCC Metals

Metal	$(v_I^f/\Omega)_{th}$	$(v_I^f/\Omega)_{exp}$
Ag	1.81	---
Al	1.86	1.9 ± 0.3
Au	1.69	---
Ca	(1.49)	---
Cu	1.75	1.55 ± 0.2
Ir	(2.26)	---
Ni	1.85	1.8 ± 0.3
Pb	1.63	---
Pd	1.4	---
Pt	1.9	1.8 ± 0.3
Rh	(2.13)	---
Sr	(1.41)	---
Th	1.75	---
Yb	(1.46)	---
Ni ₃ Fe	---	1.45 ± 0.3
NiCu	---	1.6 ± 0.3

Values in parenthesis are based on estimates for the pressure derivative of the shear modulus. Experimental values as given by Ehrhart [6].

Table II. Relaxation Volumes for Self-Interstitial in BCC Metals

Metals	$(v_I^f/\Omega)_{th}$	$(v_I^f/\Omega)_{exp}$
Cr	(0.88)	---
Cs	(0.80)	---
α -Fe	0.91	1.1 ± 0.2
K	0.76	---
Li	0.70	---
Mo	0.85	1.1 ± 0.2
Na	0.76	---
Nb	0.76	---
Rb	0.75	---
Ta	0.78	---
V	(0.77)	---
W	0.92	---

Values in parenthesis are based on estimates for the pressure derivative of the shear modulus. Experimental values as given by Ehrhart [6].

Table III. Measured Volumes Associated with Vacancies in FCC and BCC Metals

Metal	$\Delta V_V^S/\Omega$	$\Delta V_V^f/\Omega$
Ag	0.9	0.95
Al	0.71, 1.3	---
Au	0.72	0.85
Cu	0.9	0.75
Ni	---	0.8
Pb	0.73	---
Pt	---	0.8
Fe-Ni	0.86 to 0.96	---
Ni ₃ Fe	---	0.85
α -Fe	---	~ 0.75
K	0.57	---
Li	0.28	---
Mo	---	~ 0.75
Na	0.32 to 0.59	---

Relaxation Volumes for Vacancies

Although the activation volume ΔV_V^S for self-diffusion can be simply determined by measuring self-diffusion as a function of pressure, there are only a few measurements available as compiled recently by Peterson [9] for pure metals. Experimentally determined values for the vacancy formation volume, ΔV_V^f , are equally few in number, and they have recently been reviewed by Ehrhart [6]. Table III provides a list of these values together with two additional parameters for fcc binary alloys of iron and nickel. The range of values for the Fe-Ni alloys is due to Goldstein et al. [10], whereas the value for the ordered alloy Ni₃Fe is due to Ehrhart [6]. It is reassuring to see that the formation and the activation volumes for the alloys are quite similar to the values in the pure metals of the same structure. Furthermore, the formation and the activation volumes are comparable in magnitude, implying that in fcc metals and alloys, $|\Delta V_V^S/\Omega|$ is on the order of 0.1.

Unfortunately, no clear trend seems to emerge yet for the bcc metals except that the alkali metals exhibit low values for activation volume $\Delta V_V^S/\Omega$. Let us therefore consider a theoretical approach to evaluate $\Delta V_V^S/\Omega$.

Sherby et al. [11] have proposed semi-empirical correlations for both the activation energy and volume for self-diffusion. According to their analysis, self-diffusion energies can be related to the melting temperature T_M as

$$Q = kT_M(\kappa + \psi) \quad (5)$$

where k is the Boltzmann constant, κ is a crystal structure factor ($\kappa = 14$ for bcc, $\kappa = 17$ for fcc) and ψ is the valence of the element. For the activation volume, the relationship

$$\Delta V_V^S = k(\kappa + \psi)\Delta V_M/\Delta S_M \quad (6)$$

is obtained based on the assumption that the activated state of the saddle-point configuration forms a liquid-like cluster. Here ΔV_M and ΔS_M are the volume and the entropy change upon melting, respectively. Evaluating the activation volume with Eq. (6), Sherby et al. [11] conclude that $\Delta V_V^S/\Omega$ is about 0.8 for fcc crystals (except noble gases), 0.6 for hcp crystals, and 0.4 for bcc crystals.

We can combine Eqs. (5) and (6), obtain

$$\Delta V_V^S = (Q/T_M)(\Delta V_M/\Delta S_M) \quad (7)$$

and then use only experimental values to determine ΔV_V^S . The activation energies, Q , were obtained from a recent compilation by Peterson [9], and all other parameters are from the compilation by Turkdogan [12]. Melt volume changes for γ -Fe were obtained by extrapolating the temperature dependence of the molar volume [13] for γ -Fe up to the melting point. For the bcc metals Cr, Mo, Nb, and W no melt volume changes are available, and an average value of 4% was assumed in this case. Several metals exhibit different activation energies for self-diffusion for low and for high temperatures [9]. Therefore, Eq. (7) is evaluated for both values. The various parameters used and the results are shown in Table IV separated into groups of fcc and bcc metals.

With the exceptions of Ag and Li, the computed values for $\Delta V_V^S/\Omega$ are in fair agreement with the measured values. The computed value of the activation volume for δ -Fe is less than the value of 0.95 estimated by Ehrhart for ΔV_V^f from the experimental result for α -Fe. The computed value of 0.55 for ΔV_V^S in Mo is also smaller than the measured range for ΔV_V^f . Although this comparison is questionable because of the uncertain nature of Eq. (7), the following trends are suggested.

ΔV_V^S for bcc crystals is indeed somewhat less than the corresponding value in fcc crystals, although the difference is not always as large as Sherby et al. [11] claimed. The alkali metals do have low values of ΔV_V^S but they may not be representative of other bcc metals. Based on the only two cases available, the

Table IV. Computed Activation Volumes for Self-Diffusion in FCC and BCC Metals

Metal	T_M (°K)	ΔS_M (cal/ mol)	$\Delta V_M/\Omega$ (%)	Q (kcal/ mol)	$\Delta V_V^S/\Omega$
Ag	1234	2.19	3.405	40.6	0.51
				50.5	0.64
Al	933	2.76	6.99	29.5	0.80
				36.3	0.99
Au	1336	2.25	5.48	40.6	0.74
Cu	1356	2.3	3.94	54.6	1.00
				47.7	0.60
γ -Fe	(1809)	1.82	4.737	59.7	0.75
Ni	1726	2.42	6.33	67.86	0.98
				66.4	1.01
Pb	601	1.91	3.80	85.3	1.29
				26.1	0.86
Pt	2042	2.3	6.61	68.2	0.96
Cr	2130	1.9	(4.0)	73.7	(0.73)
δ -Fe	1809	1.82	3.92	56.9	0.68
K	336	1.66	2.54	9.75	0.44
Li	381	1.58	2.78	12.0	0.56
				15.9	0.74
Mo	2903	2.3	(4.0)	92.2	(0.55)
Na	370	1.67	3.25	8.41	0.44
				10.60	0.56
Nb	2750	2.34	(4.0)	96.0	(0.59)
W	3673	2.3	(4.0)	153.0	(0.72)

computed values for ΔV_V^S are smaller than the values for ΔV_V^f as estimated from experimental results [6] for the bcc metals α -Fe and Mo. It then appears possible that for bcc metals $\Delta V_V^S < \Delta V_V^f$, and a large negative relaxation volume as suggested by Sherby et al. [11] may be associated with the saddle-point configuration of the vacancy as a result of the more open bcc lattice structure.

Recent computer simulation results by Baskes [14] for ΔV_V^S in α -Fe gave a value of 0.49 Ω , confirming a large relaxation volume of -0.51 Ω for vacancies in the saddle-point configuration.

3. Net Bias

Void nucleation as well as growth depends critically on the net bias. As shown by Si-Ahmed and Wolfer [14] this net bias for a void containing x vacancies can be defined as

$$B(x) = \frac{\langle Z_1 \rangle}{\langle Z_V \rangle} - \frac{A_0(x)Z_1^0(x)}{A_0(x-1)Z_V^0(x-1)} \quad (8)$$

where $A_0(x)$ is the surface area of the void, and

$Z_I^0(x)$ and $Z_V^0(x)$ are the void bias factors for interstitials and vacancies, respectively. The sink-averaged bias factors $\langle Z_I \rangle$ and $\langle Z_V \rangle$ can be assumed to be equal to the dislocation bias factors Z_I^d and Z_V^d if dislocations represent the predominant sink. For the early stage of nucleation this is certainly the case. For large vacancy clusters with $x > 10$ the difference between $A_0(x-1)$ and $A_0(x)$ and between $Z_V^0(x-1)$ and $Z_V^0(x)$ may be neglected, and we can define the net bias as

$$B(x) \equiv \frac{Z_I^d}{Z_V^d} - \frac{Z_I^0(x)}{Z_V^0(x)} \quad (9)$$

which then agrees with the definition of the net bias for void growth.

Void Bias Factors

If $U(r)$ represents the interaction energy of the point defect with the void, then the void bias factors can be computed from the following expression [15]

$$Z^0(a) = \left\{ \int_0^1 d\left(\frac{a}{r}\right) \exp[U(r)/kT] \right\}^{-1} \quad (10)$$

for a void of radius a , where $a = (3\Omega x/4\pi)^{1/3}$. For voids without an associated segregation shell, the interaction energy is given by

$$U(r) = -\frac{\Gamma}{a^3} \left[\left(\frac{r}{a} - 1\right)^3 + \alpha_0 \left(\frac{r}{a} - 1\right)^6 \right]^{-1} + \frac{3\alpha^G}{8\mu^2} \frac{a^6}{r^6} \left(p - \frac{2\gamma}{a}\right)^2 \quad (11)$$

Here, the first term represents the image interaction [16] with the void surface, and it depends on the parameters

$$\Gamma = \mu\nu^2 \frac{(1+\nu)^2}{36\pi(1-\nu)}, \quad \alpha_0 = (7-5\nu)/30 \quad (12)$$

where μ is the shear modulus, ν is the Poisson's ratio, and ν is the relaxation volume of the point defect. The second term constitutes the modulus interaction [16], and it depends on the shear polarizability α^G of the point defect and on the effective pressure $(p - 2\gamma/a)$ on the void surface. Here, p is the gas pressure in the void and γ is the surface tension.

For very small voids with radii a approaching atomic dimensions, it can be shown that the far-field image interaction becomes equal to a modulus interaction of a vacancy with the stress field of a point defect. The vacancy is modeled in this context as an inhomogeneous inclusion whose bulk and shear moduli are zero. The shear polarizability of such a vacancy or void is given by

$$\alpha_{\text{void}}^G = -\mu \frac{4\pi}{3} a^3 \frac{15(1-\nu)}{7-5\nu} \quad (13)$$

and its relaxation volume by

$$\delta V = \frac{4\pi}{3} a^3 \frac{9(1-\nu)}{4\mu(1+\nu)} \left(p - \frac{2\gamma}{a}\right) \quad (14)$$

Based on this interpretation, we may include the second term in Eq. (11) into the first term and write

$$U(r) \equiv -\frac{\Gamma}{a^2} \left[\left(\frac{r}{a} - 1\right)^3 + \lambda \left(\frac{r}{a} - 1\right)^6 \right]^{-1} \quad (15)$$

$$\text{where } \lambda = \alpha_0 - \frac{\Gamma}{a^3} \frac{8\mu^2}{3\alpha^G(p - 2\gamma/a)^2} \quad (16)$$

The interaction energy $U(r)$ varies strongly with the distance r from the void center. With increasing r , the variation is in fact proportional to $(a/r)^6$. Therefore, the factor $\exp[U/kT]$ in the integral of Eq. (10) is practically one for large distances r . For short distances, however, $U(r)$ assumes large negative values, and the integrand becomes zero. As a result we may use the following approximation

$$\int_0^1 d\left(\frac{a}{r}\right) \exp[U(r)/kT] \approx \int_0^{a/r_c} d\left(\frac{a}{r}\right) = \frac{a}{r_c} \quad (17)$$

where r_c is defined as that distance for which the integrand drops precipitously, i.e.

$$\exp[U(r_c)/kT] = \frac{1}{f} \quad (18)$$

where $1/f$ is around $1/2$. Equation (18) can be solved for r_c/a which then according to Eq. (10) is equal to the void bias,

$$Z^0(a) \approx \frac{r_c}{a} = 1 + \left[\frac{\sqrt{1+n} - 1}{2\lambda} \right]^{1/3}, \quad (19)$$

$$\text{where } n = 4\lambda\Gamma/[a^3kT \ln f] \quad (20)$$

The void bias obtained with Eq. (19) compares very favorably with earlier results for which the integration in Eq. (10) was carried out numerically [15]. Furthermore, the results of Eq. (19) are insensitive to the choice of the parameter f as long as $(1/f)$ is not too close to either 0 or 1. Table V demonstrates this insensitivity to the choice of f for the void bias factor ratio of a "void" with radius equal to the Burger's vector. The reason for this insensitivity is that $\exp(U/kT)$ exhibits a very sharp transition from values close to one to very small values at $r \approx r_c$.

Table V. Sensitivity of the Void Bias* to the Parameter f

f	1.1	1.2	1.5	2.0	4	10
$Z_I^0(b)/Z_V^0(b)$	1.734	1.743	1.742	1.730	1.697	1.660

*For 500°C, $\nu_I = 1.4$, $\nu_V = -0.2$, $\alpha_I^G = \alpha_V^G = 0$

Dislocation Bias Factors

The interaction energy of point defects with edge dislocations has been treated extensively by Wolfer and Ashkin [16]. The dominant long-range size interaction is given by

$$U_1^d(r, \phi) = -B_0 \cos \phi / r \quad (21)$$

where
$$B_0 = v \frac{ub}{3\pi} \frac{1+v}{1-v} \quad (22)$$

and ϕ is the angle of the radius vector \vec{r} with the normal vector of the glide plane. At short distances, the modulus interaction becomes dominant, and it is given by

$$U_2^d(r, \phi) = (A_0 + A_2 \cos 2\phi) / r^2 \quad (23)$$

where

$$A_0 = [\alpha^K (1-2\nu)^2 + \frac{4}{3} \alpha^G (1-\nu + \nu^2)] / [4\pi(1-\nu)]^2 \quad (24)$$

and

$$A_2 = [(\alpha^K - \frac{2}{3} \alpha^G)(1-2\nu)^2 + 4\alpha^G \nu(1-\nu)] / [4\pi(1-\nu)]^2 \quad (25)$$

The bulk polarizabilities, α^K , of point defects are small in comparison to the shear polarizabilities, and they have been neglected in the present study.

Using a Poisson's ratio of $\nu = 0.3$ one finds that

$$A_0 = 0.0136 \alpha^G$$

$$A_2 = 0.0094 \alpha^G$$

Therefore, A_0 is the dominant term, and the term $A_2 \cos 2\phi$ merely represents an angular modulation of the dominant attractive part of the modulus interaction. On average, we may therefore use the approximation

$$U_2^d(r, \phi) \cong A_0 / r^2 \quad (26)$$

To evaluate the dislocation bias factor, the crystal around an edge dislocation can be divided into three regions. In the core region $r < c$, the modulus interaction U_2^d is so strong that its radial variation over a distance b exceeds the migration energy E^m of the point defect; i.e.

$$b \frac{dU_2^d}{dr} > E^m \quad (27)$$

The condition for equality then defines the capture radius c at which no further thermal activation is required for the point defect to migrate into the dislocation core region.

Next to the core region, there exists a region $c < r < d$, in which U_2^d is still dominant. In the outermost region, the size interaction U_1 becomes dominant and U_2^d can be neglected. However, since both interactions have an angular dependence, the radial

distance d depends in fact on the angle.

In the present study, we have therefore selected the minimum distance d , which occurs in the direction where U_1^d exhibits a maximum, i.e. for $\phi = \pm\pi/2$, depending on the sign of the relaxation volume v . Accordingly,

$$d = b^2 |A_0 - A_2| / |B_0| \quad (28)$$

By solving a steady-state diffusion equation in the two outer regions and matching the solutions approximately at $r = d$, the following equation is obtained for the dislocation bias factor:

$$Z^d = \ln(R/c) / (Q_1 - Q_2) \quad (29)$$

Here, $2R$ is the average distance between dislocations and

$$Q_1 = \frac{K_0(r_0/R)}{I_0(r_0/R)} - \frac{K_0(r_0/d)}{I_0(r_0/d)} \quad (30)$$

and

$$Q_2 = \frac{1}{2} \exp(r_2^2/d^2) I_0^{-2}(r_0/d) [E_1(r_2^2/d^2) - E_1(r_2^2/c^2)] \quad (31)$$

Here

$$r_0 = |B_0/2kT| \quad (32)$$

$$r_2^2 = |A_0/kT| \quad (33)$$

$I_0(x)$ and $K_0(x)$ are the modified Bessel functions of zero-th order and $E_1(x)$ is the exponential integral.

4. Results

The bias factor formulae derived in the previous section have been numerically evaluated to obtain the net bias parameter of Eq. (9) for various void radii. The materials parameters used were those for nickel, and the point defect parameters were

$$\alpha_I^G = -2.4 \times 10^{-17} \text{ J},$$

$$\alpha_V^G = -2.4 \times 10^{-18} \text{ J}$$

$$v_I/\Omega = 0.7 \text{ to } 2.2,$$

$$v_V/\Omega = -0.5 \text{ to } -0.1.$$

In order to simulate austenitic alloys, it was assumed that the shear polarizabilities are the same as those for nickel, whereas the relaxation volumes were assumed to be $v_I/\Omega = 1.8$ and $v_V/\Omega = -0.1$ in accordance with the results of Tables I and III.

For ferritic alloys, it was assumed that $v_I/\Omega = 1.1$ and $v_V/\Omega = -0.5$. The difference in shear moduli, atomic volumes, in shear polarizabilities, and in Burger's vectors between austenitic and ferritic alloys was neglected in the present study, and the same surface energy of $\gamma = 1 \text{ J/m}^2$ was selected for both materials. The net bias differences displayed in Fig. 2 is therefore entirely due to the differences in the relaxation volumes.

The results in Fig. 2 demonstrate the following important findings. The net bias of small voids is negative, indicating a preferential absorption for interstitials even in the presence of dislocations. Therefore, for voids to nucleate, either segregation and/or internal gas pressure is required. For larger void sizes with diameters visible in the electron microscope, the net bias is positive and voids continue to grow. If a positive net bias of 0.2 is required for nucleation to occur, then ferritic alloys are seen to exhibit a much greater resistance than austenitic alloys.

For void diameters greater than 20 nm, the net bias reaches a constant value. This value is substantially larger in austenitic alloys as compared to ferritic alloys. Figure 3 shows this asymptotic value of the net bias as a function of the relaxation volumes of both the self-interstitial and the vacancy. The most probable range for the net bias in ferritic and austenitic alloys is also indicated.

5. Discussion

It may appear that a net bias of the order of one, as displayed in Figs. 2 and 3 for the austenitic alloys, is too large in comparison to previously reported values in the literature. Therefore, the corresponding steady-state swelling rate may appear to be excessive. However, as shown below, this is not the case.

Wolfer and Garner [17] have shown that the steady state swelling rate can be expressed as

$$\frac{d}{dt} \frac{\Delta V}{V} \approx \frac{S_0 S_d}{(S_0 + S_d)^2} B \cdot F \quad (34)$$

where S_0 and S_d are the sink strength of voids and dislocations respectively, and F is a function weakly dependent on temperature and total sink strength, but strongly dependent on the rate of point defect production, P , which can be written as

$$P = \beta \dot{D} \quad (35)$$

where \dot{D} is the displacement rate and β is the fraction of point defects which survive in-cascade recombination and clustering. β is of the order of 0.1.

We may now express the swelling rate in units of (%/dpa) and write Eq. (34) as

$$\frac{d(\Delta V/V\%)}{d(\text{dpa})} = \frac{S_0 S_d}{(S_0 + S_d)^2} 100 \beta B (F/P) \quad (36)$$

As previously shown [17], $F/P < 1/2$. Furthermore, the factor

$$\frac{S_0 S_d}{(S_0 + S_d)^2} < \frac{1}{4} \quad (37)$$

where the equal sign holds when the void sink strength equals the dislocation sink strength.

Using these upper bounds and the value $\beta = 0.1$ we find that

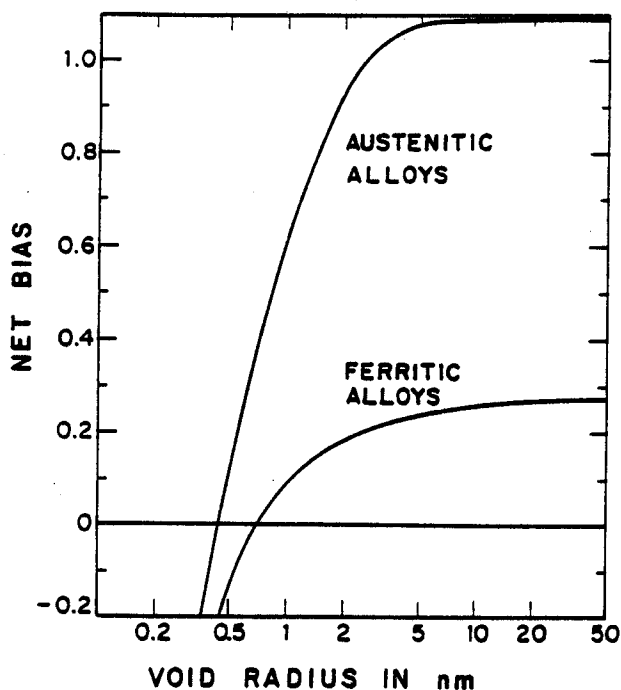


Fig. 2. Net bias for voids in austenitic and ferritic alloys.

$$\frac{d(\Delta V/V\%)}{d(\text{dpa})} < 1.25 B \text{ (\%/dpa)} \quad (38)$$

Based on the net bias results of Fig. 3, we expect therefore that the swelling rate in austenitic alloys is less or equal to about 1.4 (%/dpa). This value is remarkably close to the empirical value of 1 (%/dpa) found for the steady-state swelling rate in type 304 and 316 stainless steels. Our present assessment of the steady-state swelling rate in ferritic steels indicates that it should be lower by a factor of two to ten compared to the austenitic steels.

This large uncertainty is based on the relatively wide error band associated with the measured relaxation volume for the self-interstitial in α -Fe. This error band is however caused in turn by the fact that the relaxation volume v_V^f for the vacancy in its stable configuration is unknown within the bounds of 0 and -0.25Ω [6]. Assuming the value of $v_V^f = 0$ implies a large interstitial relaxation volume of about 1.3Ω , whereas the assumption $v_V^f = -0.25 \Omega$ implies $v_I^f = 0.9 \Omega$. For the net bias calculations, however, one requires the relaxation volumes v_I^s and v_V^s for the saddle-point configurations. With regard to the self-interstitial, it is reasonable to assume that $v_I^f \approx v_I^s$. In contrast, for the vacancy, $v_V^s < v_V^f$, as mentioned above. The choice of $v_I^s = 0.9 \Omega$ and $v_V^s = -0.5 \Omega$ appears then to be a realistic one, and it results in a net bias of about 0.18. From Eq. (38), a maximum possible swelling rate of 0.225%/dpa is then pre-

NET BIAS FOR LARGE VOIDS

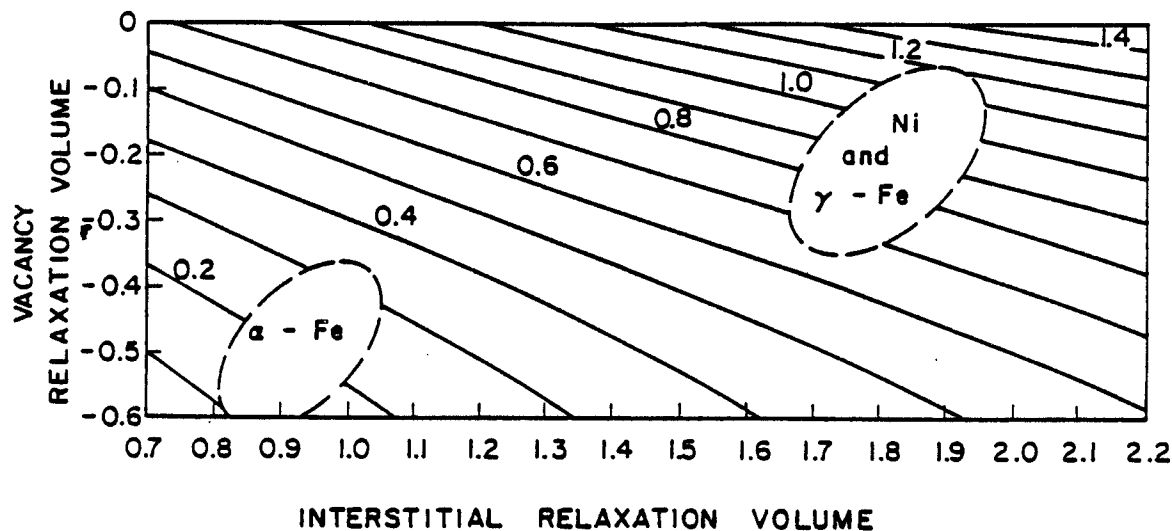


Fig. 3. Net bias as a function of the relaxation volume.

dicted. The ion-bombardment results shown in Fig. 1 on the binary alloy 85Fe-15Cr indicate a maximum swelling rate of about 0.13%/dpa.

Acknowledgement

This research has been supported by the Office of Fusion Energy, U.S. Department of Energy, under contract DE-AC02-82ER50282 with the University of Wisconsin.

References

1. F.A. Garner and D.L. Porter, "Factors Influencing the Swelling of 300 Series Stainless Steels," DAFS Quarterly Progress Report DOE/ER-0046/9, May 1982, p. 170.
2. P.J. Maziasz and M.L. Grossbeck, J. Nucl. Matls., **103 & 104**, 987 (1981).
3. H.R. Brager and F.A. Garner, J. Nucl. Matls., **103 & 104**, 993 (1981).
4. W.G. Johnston, T. Lauritzen, J.H. Rosolowski, and A.M. Turkalo, "Void Swelling in Ferritic Alloys Bombarded with Nickel Ions," in Effects of Radiation on Materials, Proc. 11th Internat. Symp., Eds. H.R. Brager and J.S. Perrin, ASTM-STP-782, 809 (1982).
5. R.W. Powell, D.T. Peterson, M.Z. Zimmerschied, and J.F. Bates, J. Nucl. Matls., **103 & 104**, 969 (1981).
6. P. Ehrhart, Conf. on Dimensional Stability and Mechanical Behaviour of Irradiated Metals and Alloys, BNES, London, 1983, paper P17.
7. D.N. Seidman, J. Phys. F: Met. Phys., **3**, 393 (1973).
8. W.G. Wolfer, J. Phys. F: Met. Phys., **12**, 425 (1982).
9. N.L. Peterson, J. Nucl. Matls., **69 & 70**, 3 (1978).
10. J.I. Goldstein, R.E. Hanneman, R.E. Ogilvie, Trans. AIME, **223**, 812 (1965).
11. O.D. Sherby, J.L. Robbins, and A. Goldberg, J. Appl. Phys., **41**, 3961 (1970).
12. E.T. Turkdogan, Physical Chemistry of High Temperature Technology, Academic Press, New York, 1980, Table 1.2 and Table 3.5.
13. W. Hume-Rothery, The Structures of Alloys of Iron, Pergamon Press, Oxford, 1980, p. 22.
14. M. Baskes, private communication.
15. A. Si-Ahmed and W.G. Wolfer, "Effect of Radiation-Induced Segregation on Void Nucleation," in Effects of Radiation on Materials, Proc. 11th Internat. Symp., Eds. H.R. Brager and J.S. Perrin, ASTM-STP-782, 1008 (1982).
16. W.G. Wolfer and M. Ashkin, J. Appl. Phys., **47**, 791 (1976).
17. W.G. Wolfer and F.A. Garner, "Temperature Dependence of the Swelling Rate in Austenitic Stainless Steels," DAFS Quarterly Progress Report DOE/ER-0046/12, Feb. 1983, p. 141.